Available online at www.sciencedirect.com
SCIENCE DIRECT®
Journal of Solid State Chemistry 179 (2006) 1852–1856
JOURNAL OF SOLID STATE CHEMISTRY
www.elsevier.com/locate/jssc

Rapid communication

Large magnetoresistance in a ferromagnetic cobaltite: The 12H $Ba_{0.9}CoO_{2.6}$

A. Maignan*, S. Hébert, D. Pelloquin, V. Pralong

Laboratoire CRISMAT, UMR 6508 CNRS ENSICAEN, 6 bd Maréchal Juin, 14050 CAEN Cedex 4, France

Received 31 January 2006; accepted 5 February 2006
Available online 20 March 2006

Abstract

The magnetic and transport properties of a hexagonal cobaltite related to the perovskite structure have been studied. By combining transmission electron microscopy, X-ray powder diffraction and iodometric titration, it is found that $Ba_{0.9}CoO_{2.6}$ crystallizes in the 12H structure [$P6_3/mmc$, $a = 5.6612\ (1)$ Å and $c = 28.4627(8)$ Å]. Interestingly, this compound is a ferromagnet with a Curie temperature $T_C = 50$ K and a saturation magnetization $M_S^{2.5\,K} = 1.2\mu_B$/Co. This value is smaller than expected from the effective paramagnetic moment, $\mu_{eff} = 3.7\mu_B$/Co, corresponding to an average spin $S \sim \frac{3}{2}$ per Co, from which one would expect $M_S^{exp.} = 3\mu_B$/Co. This suggests either a canted structure or a strong local magnetic anisotropy related to the crystal field of the CoO_n polyhedra. A clear transition in the electrical resistivity is found at T_C consistent with a spin scattering reduction as the sample becomes ferromagnetic. The spin–charge coupling is evidenced by the large negative magnetoresistance effect optimum near $T_C = 50$ K, with $[100 \times (\rho_{H=7\,T} - \rho_{H=0\,T})/\rho_{H=0\,T}] = -60\%$.

Keywords: Cobaltite; Oxide; Ferromagnetism; Magnetoresistance; Electron microscopy; Magnetic measurements

Due to the remarkable properties induced by their low-dimension magnetism, cobaltites are the focus of numerous studies. This is the case of 2D structures containing CoO_2 layers with hexagonal symmetry as Na_xCoO_2 and its hydrated derivatives which exhibit thermoelectric properties [1] and superconductivity [2], respectively. The hexagonal perovskites provide a second large family of cobaltites with chains of CoO_n polyhedra set on a hexagonal array [3–8]. The structures of these phases can be described by starting from that of the 2H-$BaMnO_3$ compound (see Ref. [3] and references therein). In the $ACoO_3$ perovskite, the nature of the stacking of the [AO_3] layers, cubic (*c*) or hexagonal (*h*), leads to either a 3D array of corner shared CoO_6 octahedra (“cubic” perovskite) or chains (“hexagonal” perovskite) of face shared CoO_6 octahedra, respectively. The regular alternation of cubic (*c*) and hexagonal (*h*) [AO_3] layers leads to different hexagonal polytypes and, additionally, the presence of oxygen vacancies in the cubic [$AO_{3-\delta}$] layers generates various sequences of CoO_n polyhedra. Thus, for the $BaCoO_{3-\delta}$ perovskite, in addition to the 2H-$BaCoO_3$ hexagonal perovskite [4], two other stacking sequences have been reported, the 5H [3,6] and the 12H [5] polytypes. The recent study of 5H-$Ba_5Co_5O_{14}$ [6] showed that, due to the $[ccchh]_\infty$ stacking, the chains are made of units of three face shared CoO_6 octahedra (Co_3O_{12}) with on each end a terminal corner-shared tetrahedron. The properties of the 2H and 5H polytypes are interesting since both exhibit negative Seebeck values at room temperature indicating that electrons dominate the transport [6,7] in contrast to the positive values reported in 2D phases containing hexagonal cobalt planes, such as Na_xCoO_2 [1] and “misfit” cobaltites [9], and also in 1D $A_{n+2}Co_{n+1}O_{3n+3}$ phases (A = alkaline-earth) [10]. Furthermore, the $Ba_5Co_5O_{14}$ phase is ferromagnetic ($T_C = 47$ K) with a refined magnetic moment per cobalt of $3.7\mu_B$ deduced from neutron powder diffraction [6]. Such a magnetic behavior differs from that of the 2H-$BaCoO_3$ compound which exhibits much smaller magnetization values [7].

*Corresponding author. Fax: +33 231 95 1600.
E-mail address: antoine.maignan@ensicaen.fr (A. Maignan).

0022-4596/$ - see front matter © 2006 Elsevier Inc. All rights reserved.
doi:10.1016/j.jssc.2006.02.010

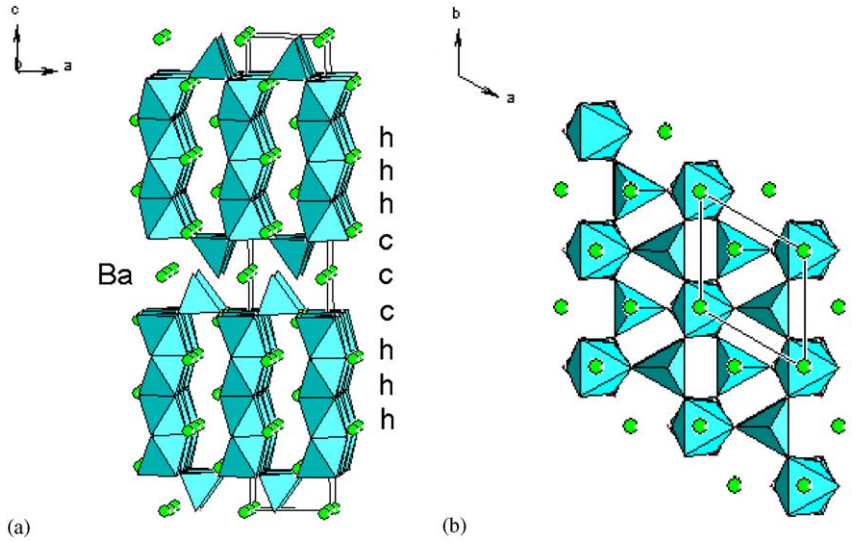

Fig. 1. Structural model of 12H hexagonal $(ccchhh)_2$ $BaCoO_{2.6}$ perovskite showing the (a) CoO_6 octahedra and CoO_4 tetrahedra. (b) Projection in the (a,b) plane.

The major difference between the 2H and 5H polytypes is the presence in the latter of different kinds of CoO_n polyhedra. The presence of tetrahedra in $Ba_5Co_5O_{14}$ is believed to break the electronic transport along the CoO_n chains in comparison to the 2H-$BaCoO_3$ phase explaining the larger resistivity of the former [6]. In that respect, the 12H-$BaCoO_{2.6}$ hexagonal perovskite with a 12-layers stacking sequence $(ccchhh)_2$ [5] instead of the $(ccchh)$ sequence of the 5H-$BaCoO_{2.8}$ perovskite [3,6] is also an interesting candidate. Its structure can also be described by chains made of units of four face-shared octahedra connected by terminals corner-shared tetrahedra (Fig. 1a). A projection of this structure in a perpendicular plane shows the existence of a triangular network made of the octahedra tetramers which are linked each other through tetrahedra located at the center of each triangle (Fig. 1b). The structural relationship with the 5H suggests that ferromagnetism and poor electrical conductivity are also expected in this 12H perovskite. The strong interplay between charges and spins in cobaltites points towards magnetoresistance (MR) properties. Nevertheless, there exists no report about such effects in the hexagonal perovskite cobaltites. This has been the motivation for the study of the 12H polytype for which no physical properties were reported. In the following, crystal data are revisited and physical properties are given for this 12H $Ba_{0.9}CoO_{2.6}$ hexagonal cobaltite.

The ceramic of 12H-$BaCoO_{3-\delta}$ was prepared by mixing stoichiometric amount of $BaCO_3$ and Co_3O_4 precursors. The mixture was then decarbonated at 900 °C for 24 h. Next it was pressed in bars ($2\times2\times10$ mm) which were heated in air at 950 °C for 120 h and then quenched in air. Finally, the sample was post-annealed at 600 °C for 12 h in a 12 MPa oxygen pressure in order to refill the possible oxygen vacancies created during the rapid cooling.

At first, the electron diffraction (ED) study of the structure by transmission electron microscopy (JEOL 200 Cx-200 kV) leads to an hexagonal cell with the unit cell parameters $a\sim5.7$ Å and $c\sim28.5$ Å, characteristic of a 12H-type hexagonal structure. The analysis of characteristic ED patterns (Fig. 2a and b) exhibits a unique condition, $hh2\bar{h}l : l = 2n$, in agreement with the space group $P6_3/mmc$ previously reported [5]. In order to confirm the crystallographic quality of the phase and the stacking sequence, high-resolution electron microscopy was also made (TOPCON 002B-200 kV). The image contrasts recorded along the $[\bar{1}010]$ direction (Fig. 2c), demonstrate the regularity of the 12 atomic layers stacking and are characteristic of a $(hhhccc)$ stacking sequence (enlarged zone in Fig. 2c). All these observations are consistent with the previous data reported for $BaCoO_{2.6}$ in Ref. [5] and the considered structural model (Fig. 1). Nevertheless, though no structural defects are observed, the energy dispersive spectroscopy (EDS) analyzes coupled to the electron diffraction observations show a systematic deviation of the cation composition leading to 0.90:1.00 for the Ba:Co ratio. By starting from the atomic positions given for this 12H structure [5], structural refinements were performed from powder X-ray diffraction data recorded at room temperature (Xpert Pro diffractometer equipped with an X' celerator detector, Cu$K\alpha$, $4^\circ\leqslant2\theta\leqslant90^\circ$, 0.0167° increment) using the Fullprof program. These refinements confirm the small Ba^{2+} deficiency (~5%) while the experimental data fitting (Fig. 3) shows best results when a small amount of 2H-$BaCoO_3$ as secondary phase (~3%) is introduced. The obtained unit cell parameters, $a = 5.6612(1)$ Å and $c = 28.4627(8)$ Å, are slightly shortened compared to $a = 5.767(1)$ Å and $c = 28.545(6)$ Å reported by Jacobson and Hutchinson for the 12H-$BaCoO_{2.6}$ phase [5]. This could be explained by the Ba^{2+} deficiency of the former. Furthermore, it must also be pointed out that these authors

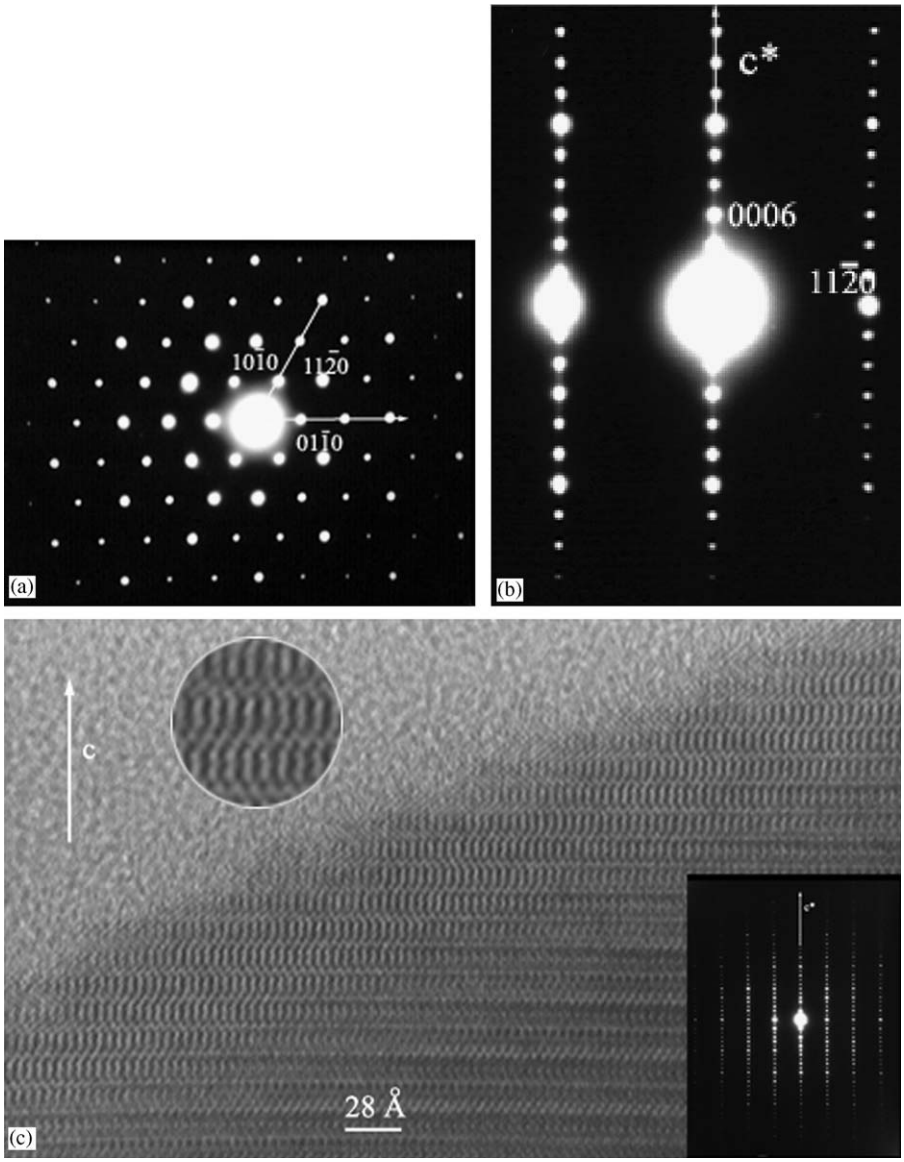

Fig. 2. Electron diffraction pattern of the $Ba_{0.9}CoO_{3-\delta}$ compound along the (a) [0001], (b) [1$\bar{1}$20], and (c) [$\bar{1}$010] directions. The corresponding experimental [$\bar{1}$010] oriented high-resolution image is shown in (c) in which the white dots can be correlated to barium rows (see enlarged zone).

observed also 2H-$BaCoO_3$ (7%) as impurity. In order to check for the cobalt oxidation state (V_{Co}), iodometric titrations were performed as described in Ref. [11]. Using the cation ratio determined by EDS, the $V_{Co} = 3.40 \pm 0.06$ value is obtained leading to the following chemical formula, $Ba_{0.9}CoO_{2.6\ (\pm 0.04)}$. No significant oxygen stoichiometry change has been detected after the second oxidizing thermal process.

The magnetic properties of the 12H-$Ba_{0.9}CoO_{2.6}$ polytype recorded with a SQUID magnetometer (Quantum Design), are illustrated in Fig. 4 by the zfc–fc magnetization curves collected in 0.3 T. A clear ferromagnetic-like transition occurs below $T_C = 50$ K with an irreversibility between the zfc and fc curves. The $\chi^{-1}(T)$ reciprocal magnetic susceptibility curve shows that $\theta_{CW} \sim 50$ K with a paramagnetic moment, $\mu_{eff} = 3.7\mu_B$/Co (Fig. 4). The former value is expected for a ferromagnet with $T_C = \theta_{CW}$ but the latter is smaller than the expected value considering a high spin state for the Co^{3+}/Co^{4+} species ($5.33\mu_B$/Co for $V_{Co} = 3.4$). The Curie temperature of $Ba_{0.9}CoO_{2.6}$ is also determined on the ac-$\chi(T)$ curves showing an abrupt appearance of the imaginary part below $T_C = 50$ K (Fig. 4b). The ferromagnetic nature found for $Ba_{0.9}CoO_{2.6}$ is confirmed by the hysteresis loops given in Fig. 5a. At 2.5 K, the magnetization increases rapidly to reach $\sim 1\mu_B$/Co in 1 T. However, the magnetization is not fully saturated but goes on increasing up to $1.2\mu_B$/Co in 5 T. A large remanent magnetization, $0.9\mu_B$/Co, is found on the reverse branch. It must be also emphasized that abrupt M reversals occur at $\pm\mu_0 H_C \sim 1$ T. This coercitive field value decreases as T increases as illustrated by the $M(H)$ curve registered just at T_C (Fig. 5b).

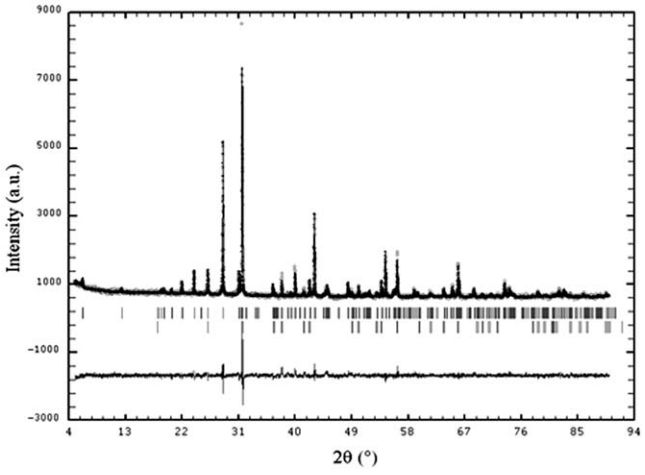

Fig. 3. Experimental (points), calculated (line) and difference X-ray powder diffraction pattern of $Ba_{0.9}CoO_{2.6}$. The second set of indexation is related to the 2H-$BaCoO_3$ phase.

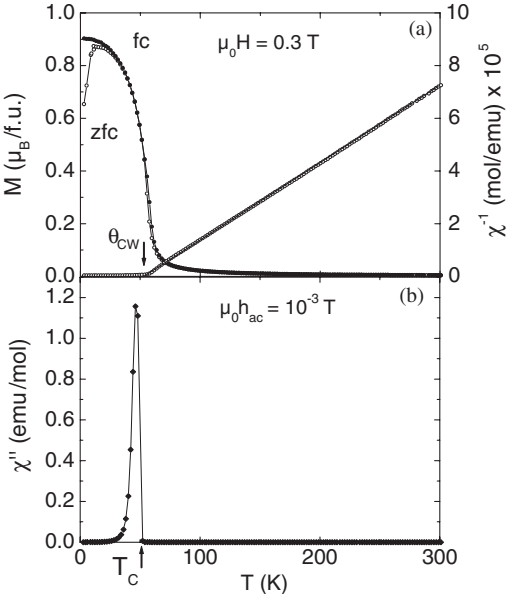

Fig. 4. (Top panel) dc magnetization as a function of T recorded in 0.3 T (zfc and fc curves) for the 12H-$Ba_{0.9}CoO_{2.6}$ hexagonal perovskite. The corresponding $\chi^{-1}(T)$ curve is also given (right y-axis); the solid line indicates the Curie–Weiss linear fitting ($\chi = C/(T-\theta_{CW})$). (Bottom panel) T-dependent ac magnetic susceptibility of the 12H-$Ba_{0.9}CoO_{2.6}$ polytype (χ'', imaginary part).

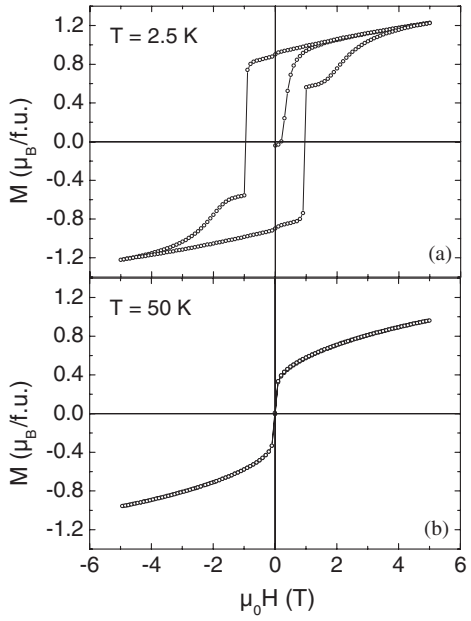

Fig. 5. Isothermal magnetic field-dependent magnetization curve of $Ba_{0.9}CoO_{2.6}$ (2.5 and 50 K in the upper and lower panels).

According to the report on the 5H-$BaCoO_{2.8}$ phase [6], the oxygen vacancies were thought to create CoO_n polyhedra with n smaller than 6, that break the CoO_6 octahedra chains found in $BaCoO_3$ creating short (CoO_6) octahedra units along the c-axis. This was invoked to explain the less conducting behavior of the 5H. The resistivity values at 400 K, $\rho = 0.1\,\Omega$ cm and $\rho = 1\,\Omega$ cm for 2H-$BaCoO_3$ [7] and 12H-$Ba_{0.9}CoO_{2.6}$ (Fig. 6), respectively, confirm this trend with a more pronounced localized character for the latter. Interestingly, at the transition temperature (T_C), a clear bump is detected for $Ba_{0.9}CoO_{2.6}$. Below this temperature, the resistivity (ρ) stops increasing as T decreases for about 10 K and then ρ exhibits a re-entrant behavior. The correspondence between T_C and this change in slope on the $\rho(T)$ curve can be explained by a spin scattering reduction as the sample becomes ferromagnetic. This is confirmed by comparing the resistivity curves collected in 0 and 7 T. A clear ρ decrease is induced by the magnetic field in the T_C vicinity which indicates negative MR. From the ratio $\rho_{H=0\,T}(T)/\rho_{H=7\,T}(T)$, a MR maximum is obtained at 50 K, i.e. at T_C. In ferromagnetic oxides, such as the $La_{1-x}Sr_xCoO_3$ perovskite [12], the spin scattering reduction near T_C is responsible for such negative MR. The MR of $Ba_{0.9}CoO_{2.6}$ is better seen in the inset of Fig. 6 showing the isothermal field-dependent MR curves, in which the MR is defined as $\%MR = 100\times[(\rho_H - \rho_{H=0})/\rho_{H=0}]$. An optimum value, MR = −60%, is obtained at 50 K in 7 T for $Ba_{0.9}CoO_{2.6}$ (Fig. 6). This MR effect at T_C shows a very large $d\rho/dH$ slope at low magnetic field, reaching already −20% in 0.5 T. In contrast, this initial slope is very small beyond T_C the compound becoming less easily magnetized.

The present study shows that the oxygen deficient $Ba_{0.9}CoO_{2.6}$ crystallizes in a 12H hexagonal structure with a Ba/Co < 1 ratio confirmed by EDS and structural refinements. This oxide is ferromagnetic with $T_C = 50$ K, i.e. a value similar to that of the 5H-$BaCoO_{2.8}$ term. However, the saturation magnetization of the present 12H is lower than that of the 5H. From the value $\mu_{eff} = 3.7\mu_B$/Co, corresponding to an average spin of $S \sim \frac{3}{2}$, one would expect a magnetization saturation (M_S) at $3\mu_B$/Co for $T \ll T_C$. Nonetheless, a canting was invoked in the 5H case to explain the difference between the average refined

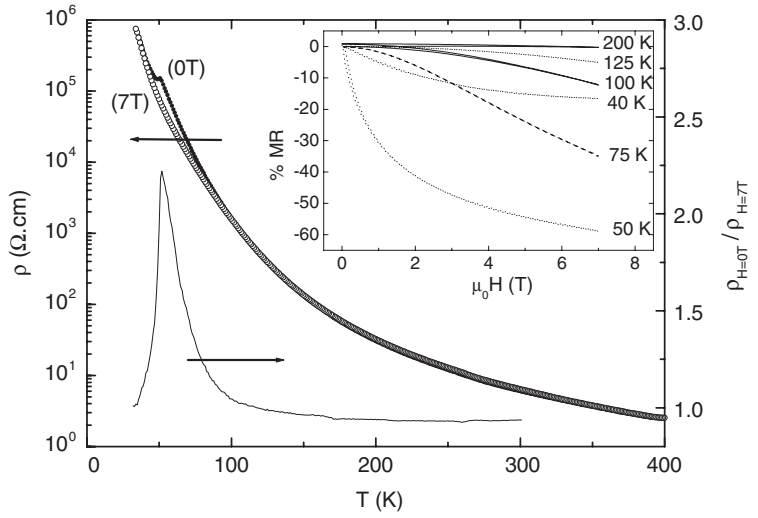

Fig. 6. T-dependent resistivity (ρ) data collected upon cooling in 0 T (filled symbols) and 7 T (open symbols). The $[\rho_{H=0}/\rho_{H=7\,T}](T)$ curve is also shown (right y-axis). Inset: isothermal magnetic field-dependent magnetoresistance.

magnetic moment per cobalt (from neutron diffraction data $3.7\mu_B$/Co) and M_S value, $M_S = 1.7\mu_B$/Co. Such a feature could also hold in the 12H case since the same canting angle would be necessary ($\sim 64^\circ$). However, one cannot discard a different explanation based on a strong magnetic anisotropy along the cobalt chains as in the $Ca_3Co_2O_6$ phase [13]. In that case, the magnetization would be very anisotropic and thus the measured magnetization along the applied magnetic field direction in such isotropic polycrystalline ceramic is the magnetizations sum of all microcrystals projected along the axis of measurements. In that case a factor of two between the M_S values of the crystal and polycrystal is calculated [M_S (crystal) $= 2M_S$ (polycrystals) [14]]. Taking $S \sim \frac{3}{2}$ as an average spin number per cobalt, one obtains M_S (polycrystal) $= 1.5\mu_B$/Co which is close to the experimental value, $M_S^{exp.}(2.5\,K) = 1.2\mu_B$/Co. Finally, the existence of a ρ bump at T_C supports the strong coupling between charges and spins in this oxide. To our knowledge, this is the first observation of a large negative MR in the hexagonal perovskites. According to the large number of members belonging to this structural family, they deserve a detailed investigation of their physical properties.

References

[1] I. Terasaki, Y. Sasago, K. Uchinokura, Phys. Rev. B 56 (1997) R12685.
[2] K. Takada, H. Sakurai, E. Takayama-Murimachi, F. Izumi, R.A. Dilanian, T. Sasaki, Nature 422 (2003) 53.
[3] M. Parras, A. Varela, H. Seehofer, J.M. Gonzales-Calbet, J. Solid State Chem. 120 (1995) 327.
[4] H. Taguchi, Y. Takeda, F. Kanamaru, M. Shimada, M. Koizumi, Acta Crystallogr. Cryst. Chem. B 83 (1977) 1299.
[5] A.J. Jacobson, J.L. Hutchison, J. Solid State Chem. 35 (1980) 334.
[6] K. Boulahya, M. Parras, J.M. Gonzalez-Calbet, U. Amador, J.L. Martinez, V. Tissen, M.T. Fernandez-Diaz, Phys. Rev. B 71 (2005) 144402.
[7] K. Yamaura, H.W. Zandbergen, K. Abe, R.J. Cava, J. Solid State Chem. 146 (1999) 96.
[8] M. Zanne, A. Courtois, C. Gleitzer, Bull. Soc. Chim. Fr. 0 (1972) 4470.
[9] A.C. Masset, C. Michel, A. Maignan, M. Hervieu, O. Toulemonde, F. Studer, B. Raveau, J. Hejtmanek, Phys. Rev. B 62 (2000) 166.
[10] T. Takami, H. Ikuta, U. Mieutani, Jpn. J. Appl. Phys. 43 (2004) 12.
[11] B. Raveau, V. Pralong, V. Caignaert, M. Hervieu, A. Maignan, J. Phys.: Condens. Matter 17 (2005) 7371.
[12] S. Yamaguchi, H. Taniguchi, H. Takagi, T. Arima, Y. Tokura, J. Phys. Soc. Jpn. 64 (1995) 1885.
[13] A. Maignan, V. Hardy, S. Hébert, M. Drillon, M.R. Lees, O. Petrenko, D.M.K. Paul, D. Khomskii, J. Mater. Chem. 14 (2004) 1231.
[14] V. Hardy, private communication.